



Synthesis and Characterization of Novel Soluble Fulleropyrrolidine Derivatives and Their Photovoltaic Performance

Dongbo Mi and Do-Hoon Hwang*

Department of Chemistry, and Chemistry Institute for Functional Materials, Pusan National University,
Busan 609-735, Republic of Korea

Currently, [60] fullerene derivatives are the focus of considerable research due to their important roles in many fields, especially material science. In this study, we synthesized the following two novel fulleropyrrolidine derivatives: C₆₀-fused *N*-methyl-(4-hexyloxybenzen-2-yl) pyrrolidine, (*p*-HOPF) and C₆₀-fused *N*-methyl-(2-hexyloxybenzen-2-yl) pyrrolidine, (*o*-HOPF). Structural assignments of the two fullerene derivatives were made through ¹H NMR and FAB-MS. We also measured the optical and electrochemical properties of *p*-HOPF and *o*-HOPF through UV/Vis spectrophotometry and cyclic voltammetry. We found that the difference in the position of the alkoxy substituent on the phenyl ring greatly affects the characteristics of the molecules. In particular, from the ¹H NMR spectrum, we found that the hydrogen atoms on the carbons adjacent to the oxygens in *p*-HOPF and *o*-HOPF have completely different chemical environments. In order to study the effects of the substituent group positions on photovoltaic performance, photovoltaic devices were fabricated. The highest power conversion efficiency, 0.71%, was achieved when using *o*-HOPF as the electron acceptor.

Keywords: Fullerene Derivatives, Fulleropyrrolidine, 1,3-Dipolar Reaction, Photovoltaic Devices.

1. INTRODUCTION

In the two decades since [60] fullerene (C₆₀) was first isolated and produced in bulk quantities in 1985, fullerene derivatives have been developed and their organic chemistry has been successfully studied.^{1–10} Chemists have been attracted by their interesting chemistry as well as by potential applications.^{11–13} Many successful methods of functionalization have been explored, such as nucleophilic additions,¹⁴ Diels-Alder reactions,¹⁴ 1,3-dipolar and other types of cycloadditions,¹⁴ oxidations,¹⁴ halogenations,¹⁴ carbene and nitrene additions,¹⁵ hydrogenations,^{16,17} organo-transition-metal reactions,¹⁸ and others. The 1,3-dipolar cycloaddition of azomethine ylide is an efficient, easily processed, and widely applied method that produces an important class of fullerene derivatives known as the fulleropyrrolidines.

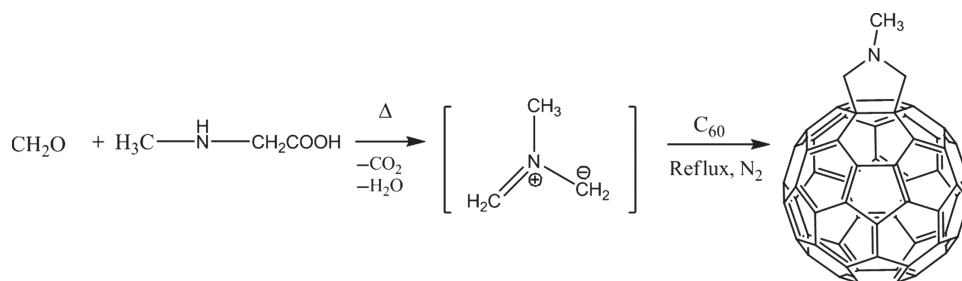
Scheme 1 shows the formation of the simplest compound of this class, *N*-methylfulleropyrrolidine to illustrate the general approach. The reactive intermediate is generated through the decarboxylation of an immonium

salt, which is formed by the condensation of an α -amino acid with an aldehyde. The intermediate is generated *in situ* and undergoes cycloaddition with [60] Fullerene, a process known as the Prato reaction. The fulleropyrrolidines that are formed each contain a pyrrolidine ring fused to a junction between two six-membered rings of a fullerene sphere.¹⁹

The key features of this reaction are as follows: (a) the reactions lead to individual [6,6]-closed isomers, and (b) the majority of precursors are commercially available or easily prepared.¹⁹ Furthermore, functionalization of the fullerene sphere through the Prato reaction is easily accomplished because two substituents (e.g., from the α -amino acid moiety and the aldehyde derivative) can be simultaneously introduced into the pyrrolidine heterocycle as shown in Scheme 1. These advantages make the Prato reaction useful for the synthesis of new fullerene derivatives.

In this study, we designed and synthesized two novel fulleropyrrolidine derivatives: C₆₀-fused *N*-methyl-(4-hexyloxybenzen-2-yl) pyrrolidine (*p*-HOPF) **2**, and C₆₀-fused *N*-methyl-(2-hexyloxybenzen-2-yl) pyrrolidine (*o*-HOPF) **4** (Scheme 2). Since solubility is an important

* Author to whom correspondence should be addressed.



Scheme 1. General synthetic route for *N*-methylfulleropyrrolidine.

prerequisite for the application of [60] fullerene derivatives in common organic semiconductor devices such as organic thin-film transistors (OTFTs), organic photovoltaics (OPVs), and devices based on light-induced intermolecular charge separation, we introduced alkoxy groups onto the benzene ring to improve the solubility. We also presumed that the electrochemical properties of [60] fullerene could be tuned; in particular, we expected that the LUMO energy level would be raised after modification because adds on the [60] fullerene core can reduce the π -conjugation length and raise the LUMO level. This change in electrochemical properties is beneficial for some applications, especially OPV devices. However, the adds inevitably change the crystal packing, typically reducing the fullerene–fullerene contact distance, and they may also reduce the carrier mobility. In order to minimize the impact on the crystal packing of [60] fullerene, we attached only hexyloxy-substituted aryl rings to the basic *N*-methylfulleropyrrolidine structure. The synthetic routes to the fulleropyrrolidine derivatives and their chemical structures are shown in Scheme 2.

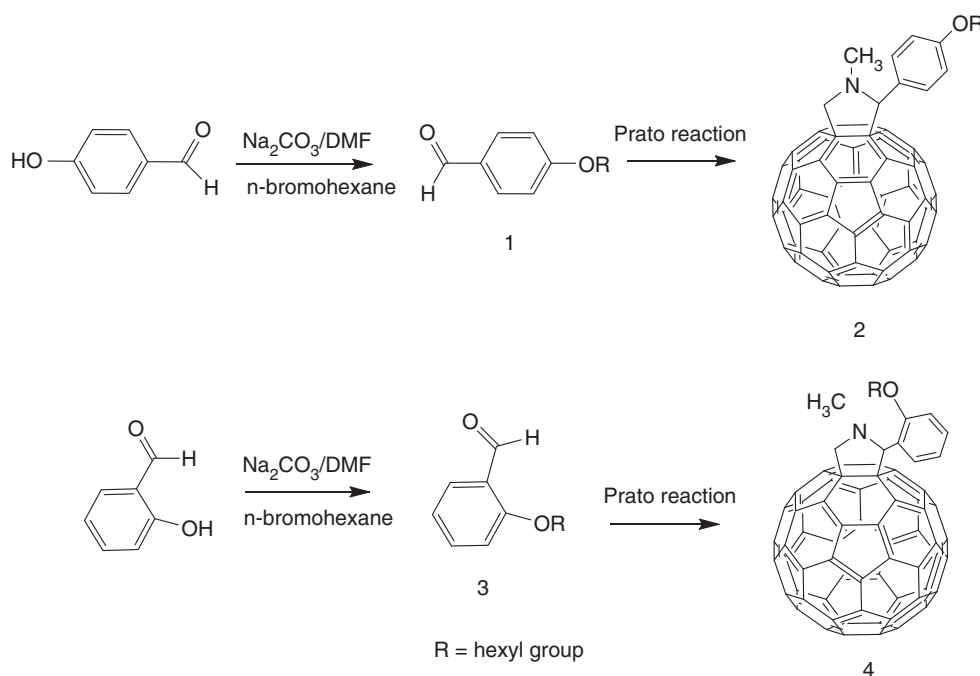
2. EXPERIMENTAL DETAILS

2.1. Materials

4-Hydroxybenzaldehyde, salicylaldehyde, sodium carbonate, *n*-bromohexane, sarcosine, 1,2-dichloroethane, 2-ethylhexylbromide, anhydrous dimethylformamide, phosphorus chloride, anhydrous *o*-dichlorobenzene, and fullerene were purchased from Alfa Aesar or Aldrich. All chemicals and solvents were analytical grade and were used without further purification.

2.2. Measurements and Device Fabrications

^1H NMR spectra were recorded using a Varian AM-300 spectrometer, absorption spectra were obtained using a Scinco S-3100 spectrophotometer, and fast atom bombardment mass spectra (FAB-MS) were measured using a JEOL-ZMS-DX-303 mass spectrometer. Cyclic voltammetry (BAS 100) was performed with a solution of tetrabutylammonium tetrafluoroborate (TBABF₄, 0.10 M) as the electrolyte and the fulleropyrrolidine material (10^{-3} M) in



Scheme 2. Synthetic routes and chemical structures of *p*-HOPF and *o*-HOPF.

1,2-dichlorobenzene; the voltammograms were collected at a scan rate of 50 mV/s, at room temperature, and under an argon atmosphere. A glassy carbon electrode (0.3 mm diameter) was used as the working electrode. Pt and Ag/AgCl electrodes were used as the counter electrode and reference electrode, respectively. Composite solutions of P3HT and the synthesized fulleropyrrolidine derivatives were prepared using chlorobenzene as the solvent. Polymer photovoltaic devices were fabricated with the typical sandwich structure of ITO/PEDOT:PSS/active layer/LiF/Al. The current voltage (I - V) characteristics of all the polymer photovoltaic cells were measured under simulated solar light (100 mW/cm²; AM 1.5 G) provided by an Oriel 1000 W solar simulator. The characterizations were carried out in an ambient environment, and electrical data were recorded using a Keithley 236 source-measure unit. The intensity of the simulated solar light was calibrated using a standard Si photodiode detector (PV measurements Inc.), which in turn was calibrated at the National Renewable Energy Laboratory (NREL).

2.3. Synthesis of *p*-HOPF and *o*-HOPF

2.3.1. Synthesis of 4-(hexyloxy)Benzaldehyde (1)

4-Hydroxybenzaldehyde (5 g, 0.04 mol) and sodium carbonate (6.57 g, 0.06 mol) were dissolved in 50 ml of DMF, and the reaction mixture was stirred for 30 min at room temperature. *n*-Bromohexane (7.39 ml, 0.053 mol) was added to the reaction mixture, and the resulting mixture was stirred for 24 h at room temperature. The reaction mixture was extracted three times using dichloromethane and brine. The organic layer was separated and dried with anhydrous magnesium sulfate, and then the solvent was removed via rotary evaporation. The crude product was purified by column chromatography to produce a yield of 83% (7 g). ¹H NMR (300 MHz, CDCl₃): δ (ppm) 9.87 (*s*, 1 H), 7.83 (*d*, 2 H), 7.00 (*d*, 2 H), 4.03 (*t*, 2 H), 1.80 (*m*, 2 H), 1.42 (*m*, 2 H), 1.32 (*m*, 2 H), 0.89 (*t*, 3 H).

2.3.2. Synthesis of C₆₀-Fused *N*-Methyl-(4-hexyloxybenzen-2-yl) Pyrrolidine (2)

A mixture of **1** (0.06 g, 0.28 mmol), [60] fullerene (0.3 g, 0.42 mmol), and *N*-methylglycine (sarcosine, 0.124 g, 1.4 mmol) was dissolved in 100 ml 1,2-dichlorobenzene. After refluxing for 24 h, the reaction was allowed to reach room temperature, the solvent was partially vacuum evaporated, and the residue was poured onto a silica gel column. The black solid obtained after chromatography (hexane/toluene eluent) was further purified by repetitive centrifugation using methanol and hexane to yield 0.15 g *p*-HOPF as a black solid (56% yield). ¹H NMR (300 MHz, CDCl₃): δ (ppm) 7.69 (*m*, 2 H), 6.95 (*d*, 2 H), 4.97 (*d*, 1 H, $J = 9$ Hz), 4.87 (*s*, 1 H), 4.25 (*d*, 1 H, $J = 9$ Hz), 3.95 (*t*, 2 H), 2.79 (*s*, 3 H), 1.77 (*m*, 2 H), 1.44 (*m*, 2 H),

1.33 (*m*, 4 H), 0.89 (*t*, 3 H). FAB-MS ($M + 1$, C₇₅H₂₃NO): calcd, 954; found, 955.

2.3.3. Synthesis of 2-(hexyloxy)Benzaldehyde (3)

Salicylaldehyde (5 g, 0.04 mol) and sodium carbonate (6.57 g, 0.06 mol) were dissolved in 50 ml of DMF, and the reaction mixture was stirred for 30 min at room temperature. *n*-Bromohexane (7.39 ml, 0.053 mol) was added, and the resulting mixture was stirred for 24 h at room temperature. The reaction mixture was extracted three times using dichloromethane and brine. The organic layer was separated and dried with anhydrous magnesium sulfate, and the solvent was removed by rotary evaporation. The crude product was purified by column chromatography, affording **3** in 75.3% yield (6.37 g). ¹H NMR (300 MHz, CDCl₃): δ (ppm) 10.52 (*s*, 1 H), 7.82 (*dd*, 1 H), 7.53 (*dt*, 1 H), 7.02 (*m*, 2 H), 4.06 (*t*, 2 H), 1.86~1.79 (*m*, 2 H), 1.50~1.37 (*m*, 2 H), 1.32 (*m*, 2 H), 0.90 (*t*, 3 H).

2.3.4. Synthesis of C₆₀-Fused *N*-Methyl-(2-hexyloxybenzen-2-yl) Pyrrolidine (4)

A mixture of **3** (0.06 g, 0.28 mmol), [60] fullerene (0.3 g, 0.42 mmol), and sarcosine (0.124 g, 1.4 mmol) was dissolved in 100 ml 1,2-dichlorobenzene. After refluxing for 24 h, the reaction was allowed to reach room temperature, the solvent was partially vacuum-evaporated and the residue was loaded onto a silica gel column. The black solid obtained after chromatography (hexane/toluene eluent) was further purified by repetitive centrifugation using methanol and hexane to yield 0.18 g *p*-HOPF **4** as a black solid (67% yield). ¹H NMR (300 MHz, CDCl₃): δ (ppm) 7.96 (*dd*, 1 H), 7.07 (*t*, 2 H), 6.89 (*d*, 1 H), 5.56 (*s*, 1 H), 4.97 (*d*, 1 H, $J = 9$ Hz), 4.31 (*d*, 1 H, $J = 9$ Hz), 4.00 (*td*, 1 H, $J = 6$ Hz), 3.72 (*td*, 1 H, $J = 6$ Hz), 2.80 (*s*, 3 H), 1.44~1.25 (*m*, 8 H), 0.88 (3 H). FAB-MS ($M + 1$, C₇₅H₂₃NO): calcd, 954; found, 955.

3. RESULTS AND DISCUSSION

The novel fulleropyrrolidine derivatives (*p*-HOPF and *o*-HOPF) displayed excellent solubility in common organic solvents such as dichloromethane, chloroform, toluene, chlorobenzene, and 1,2-dichlorobenzene. A combination of ¹H NMR and FAB-MS was used to assign the structures of the new compounds. The characteristic peaks of the fulleropyrrolidine core were observed in the ¹H NMR spectra of both *p*-HOPF and *o*-HOPF. As shown in Figure 1(a), the two protons in the pyrrolidine ring (H_c) were clearly separated.

Owing to the ² J_{HH} coupling interaction, each separated H_c was split again into a doublet with a coupling constant as high as 9 Hz, which is consistent with other reports.²⁰ Additionally, the protons H_f were clearly split into a triplet

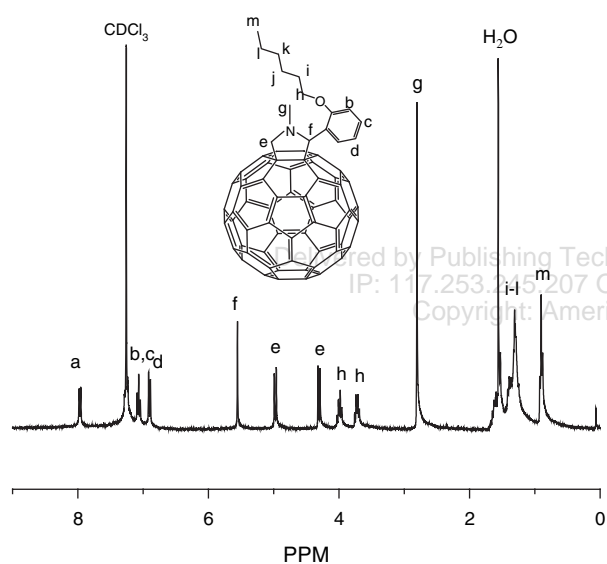
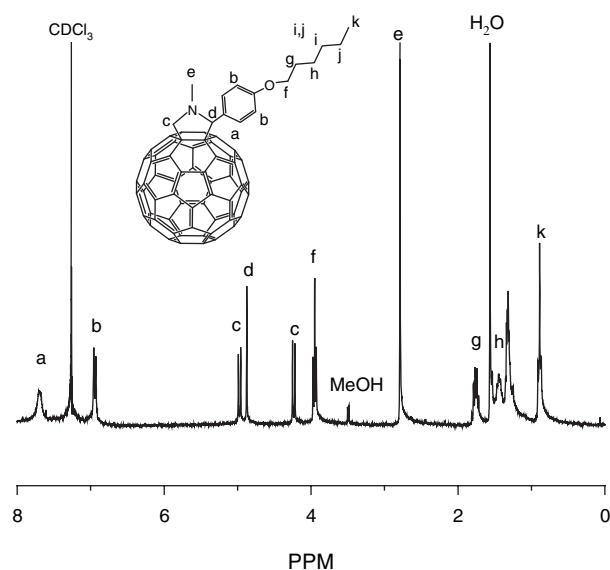


Fig. 1. (a) ^1H NMR spectrum of *p*-HOPF (2). (b) ^1H NMR spectrum of *o*-HOPF (4).

by the protons H_g . The ^1H NMR spectrum of *o*-HOPF was distinct from that of *p*-HOPF. In Figure 1(b), the two protons on the carbon adjacent to the oxygen (H_a and H_b) are separated, clearly indicating that the two protons reside in distinct chemical environments.

Focusing on H_a or H_b in *o*-HOPF, we see intuitively that each resonance is split into a doublet with a coupling constant of 9 Hz and is further split into a triplet with a coupling constant as high as 6 Hz. ($^3J_{\text{HaHb}} = ^3J_{\text{HbHi}} = 6$ Hz). This process is vividly illustrated in Figure 2(b). We attributed this phenomenon to steric hindrance between the alkoxy chain and the nitrogen methyl group. In *o*-HOPF, the methyl group and proton h (H_a or H_b) are close enough for a repulsive interaction and, because of this steric hindrance, the free rotation of the bond between O

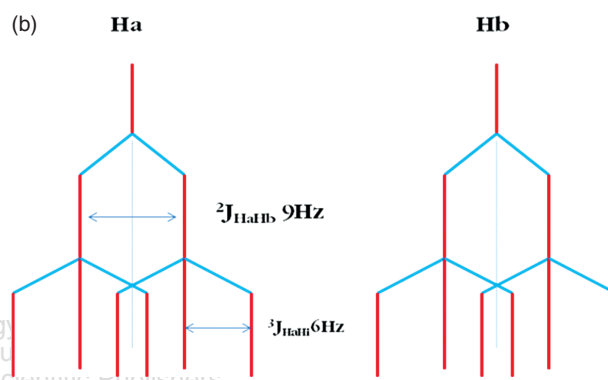
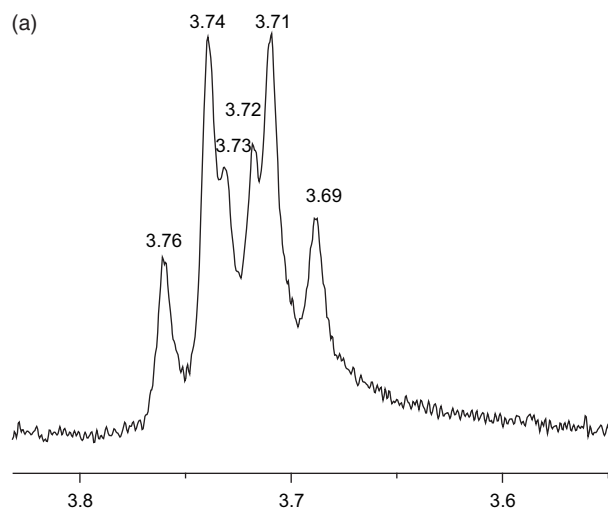


Fig. 2. (a) Expansion of ^1H NMR spectrum of *o*-HOPF in the region from 3.8 to 3.6 ppm. (b) Spin-spin splitting and coupling constants for protons H_a and H_b in *o*-HOPF.

and C_h is somewhat restricted, leaving the protons H_a and H_b inequivalent.

We recorded the UV-Vis spectra of *o*-HOPF and *p*-HOPF in 1,2-dichlorobenzene solution (10^{-5} M) to determine their optical properties. As shown in Figure 3, [60] Fullerene exhibited an absorption peak at around 330 nm. Absorption has also been observed in the long-wavelength region, as high as 900 nm (not shown); this could be considered characteristic property of fullerene-containing compounds. The absorptions of *p*-HOPF and *o*-HOPF were distinct from those of [60] Fullerene. There were no apparent absorption peaks around 330 nm, however, a broad absorption shoulder was observed around 330 nm, and the absorption intensities of these fullerypyrrolidine derivatives were much lower than that of [60] fullerene. Furthermore, the long-wavelength region contained some absorption, as shown in the inset of Figure 3, that is similar to that found in the [60] Fullerene spectrum. This further indicates the successful connection of the alkoxy phenyl moiety to the C_{60} core. Although structural modification did not improve the absorption ability of the fullerenes, it is apparent that the optical properties were significantly affected.

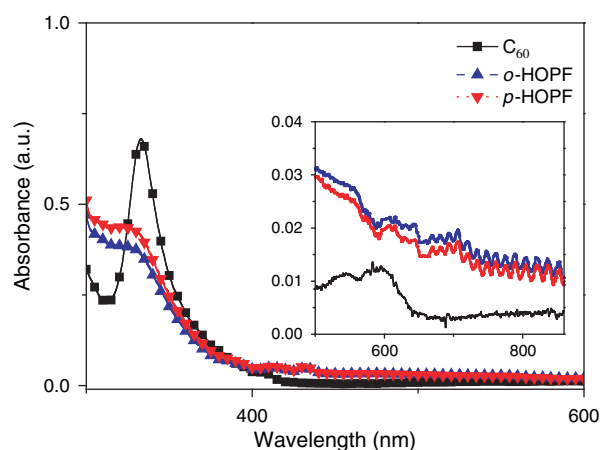


Fig. 3. UV-visible absorption spectra of [60] Fullerene, *p*-HOPF, and *o*-HOPF in 1,2-dichlorobenzene (10^{-5} M).

The electrochemical properties of fullerenes are very important: electronic energy levels (especially the LUMO level) of fullerene derivatives are crucial to their applications. Therefore, we collected the cyclic voltammograms of *p*-HOPF (**2**) and *o*-HOPF (**4**) in 1,2-dichlorobenzene solution with TBABF₄ as the electrolyte. *p*-HOPF, *o*-HOPF, and [60] Fullerene displayed multiple-quasi-reversible one-electron reduction waves, as shown in Figure 4.

These reduction waves were attributed to the fullerene core, and the first reduction potentials (E_1^{red}) were found to correspond to the LUMO energy levels of the fullerene derivatives. Both of the first reduction potentials of the novel fulleropyrrolidine derivatives were shifted to negative values with respect to the parent [60] Fullerene. This indicates that the LUMO energy levels of *p*-HOPF and *o*-HOPF are raised relative to [60] Fullerene. The measured electrochemical properties are listed in Table I. The LUMO energy levels were calculated from the onset reduction potentials ($E_{\text{Red}}(\text{onset})$) on the basis of the reference energy level of ferrocene (4.8 eV below the

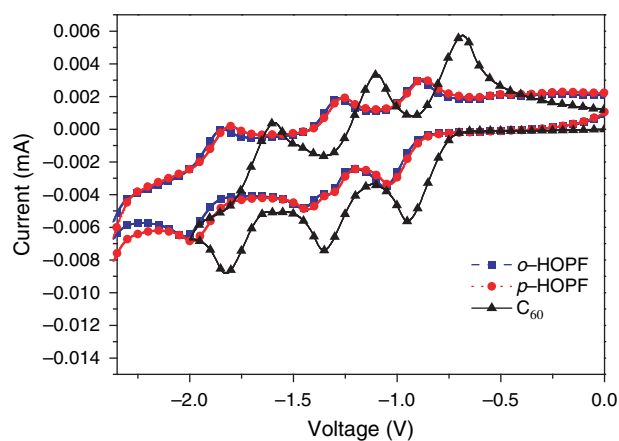


Fig. 4. Cyclic voltammograms of [60] Fullerene, *p*-HOPF, and *o*-HOPF.

Table I. Summary of electrochemical properties of [60] Fullerene, *p*-HOPF, and *o*-HOPF.

	E_{red}^1 (V)	E_{red}^2 (V)	E_{red}^3 (V)	E_{red}^4 (V)	E_{onset} (V)	LUMO (eV)
C ₆₀	-0.95	-1.35	-1.82	-	-0.76	-3.78
<i>p</i> -HOPE	-1.04	-1.31	-1.43	-1.99	-0.90	-3.65
<i>o</i> -HOPE	-1.06	-1.33	-1.46	-2.02	-0.89	-3.64

vacuum level; the vacuum level is defined as zero).^{21,22} $\text{LUMO} = -[(E_{\text{Red}}(\text{onset}) - E_{\text{foc}}) + 4.8]$ (eV), where E_{foc} is the potential of the external standard, the ferrocene/ferrocenium ion (Foc/Foc⁺) couple. The value of E_{foc} determined under the same conditions was about 260 mV versus Ag/AgCl. The values of $E_{\text{Red}}(\text{onset})$ for *p*-HOPF and *o*-HOPF were -890 and -904 mV, respectively. Thus, the LUMO energy levels of *p*-HOPF and *o*-HOPF relative to the vacuum level were estimated to be -3.65 and -3.64 eV, respectively. The LUMO energy levels of these two fulleropyrrolidine derivatives were much higher than that of [60] Fullerene (-3.78 eV) measured under the same conditions. However, there are no significant differences in the electrochemical properties of *o*-HOPF and *p*-HOPF, indicating that the substituent position of the alkoxy phenyl group has very little influence on the electronic energy levels of the C₆₀.

Recently, OPVs based on interpenetrating blends of donors and acceptors sandwiched between two asymmetric contacts (two metals with different work functions) have become very popular. Therefore, owing to their excellent solubility in common organic solvents and higher LUMO energy levels, which are beneficial for improving the open circuit voltage (V_{oc}) of photovoltaic cells, our novel fulleropyrrolidine derivatives, *p*-HOPF and *o*-HOPF, have potential as electron acceptors for the preparation of organic solar cells. Thus, photovoltaic cells were prepared with P3HT as the electron donor. In this study, we varied the weight ratio of the donor and acceptor, and we fabricated devices using different annealing temperatures and annealing times. Organic solar cells based on *o*-HOPF and *p*-HOPF as electron acceptors showed similar photovoltaic performances. Cells with *o*-HOPF as the acceptor and a composite ratio of 1:0.5 at the pristine state showed the best photovoltaic performance: a short circuit current (J_{sc}) of 0.55 mA/cm², an open circuit voltage (V_{oc}) of 0.52 V, a fill factor (FF) of 0.25, and a power conversion efficiency (PCE) of 0.71%. Figure 5 shows the photovoltaic performance of this device under AM 1.5 G illumination (intensity: 100 mW cm⁻²); the relative parameters are summarized in Table II.

The short-circuit currents and the open-circuit voltages of the devices were similar to those of devices based on P3HT/PC₆₁BM. However, the PCE was somewhat lower at the pristine state than that of the P3HT/PC₆₁BM system because of the lower FF. Unfortunately, V_{oc} and J_{sc} decreased rapidly after annealing. Furthermore, the PCE decreased even more severely when we increased the

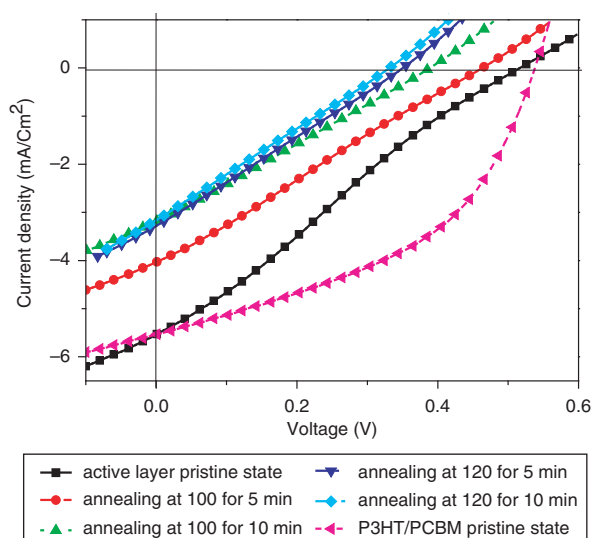


Fig. 5. Current voltage (I - V) curves of the devices with P3HT/ o -HOPF (1:0.5) after different annealing temperatures and annealing times.

Table II. Summary of photovoltaic performance of P3HT/ o -HOPF (1:0.5) devices after different annealing temperatures and annealing times.

	V_{oc} (V)	J_{sc} (mA/cm ²)	FF (%)	PCE (%)
PCBM (pristine) ^a	0.54	5.5	45.4	1.4
o -HOPF (pristine) ^b	0.52	5.5	24.9	0.71
o -HOPF(100 °C 5 min) ^b	0.46	4.0	25.1	0.47
o HOPF(100 °C 10 min) ^b	0.39	3.2	25.6	0.32
o -HOPF(120 °C 5 min) ^b	0.35	3.3	25.3	0.29
o HOPF(120 °C 10 min) ^b	0.33	3.2	24.9	0.26

Notes: ^aThe ratio of P3HT:PCBM is 1:1 w/w; ^bThe ratio of P3HT: o -HOPF is 1:0.5 w/w.

annealing temperature or extended the annealing time. The V_{oc} and J_{sc} were particularly reduced if we enhanced the ratio of p -HOPF or o -HOPF in the active layer. These observations were ascribed to the low thermal stability of the fulleropyrrolidine derivatives.

4. CONCLUSIONS

Two novel fullerene derivatives p -HOPF and o -HOPF were synthesized for the first time, and their structures were assigned using ¹H NMR and FAB-MS. Both derivatives showed good solubility in common organic solvents. We report herein the effects that the position of an alkoxyphenyl group attached to the fulleropyrrolidine core have on its optical and electrochemical properties. Given their improved solubility in common organic solvents and

ideal electrochemical properties, these new fulleropyrrolidine derivatives were evaluated to determine their potential as novel electron acceptors for donor/acceptor bulk heterojunction photovoltaic cells. Thus, we fabricated OPV cells with ITO/PEDOT:PSS/active layer /LiF/Al configurations, and the highest PCE, 0.71%, was obtained for a device based on o -HOPF. We believe that better photovoltaic performance can be achieved if we further modify the molecular structure to achieve higher thermal stability.

Acknowledgment: This research was financially supported by the Ministry of Knowledge Economy (MKE) under the New and Renewable Energy Program through a KETEP grant (No. 20103020010050 and No. 20113010010030) and by the National Science Foundation (NRF) grant funded by the Korea government (MEST) (No. 2011-0011122) through GCRC-SOP (No.2011-0030668).

References and Notes

- H. W. Kroto, J. R. Heath, S. C. O'Brien, R. F. Curl, and R. E. Smalley, *Nature* 318, 162 (1985).
- W. Kratschmer, L. D. Lamb, K. Fostiropoulos, and D. R. Huffman, *Nature* 347, 354 (1990).
- R. Taylor, *The Chemistry of Fullerenes*, World Scientific, River Edge, NJ (1995).
- K. M. Kadish and R. S. Ruoff, *Fullerene Chemistry: Physics, and Technology*, John Wiley & Sons, New York (2000).
- A. Hirsch, *The Chemistry of the Fullerenes*, Thieme, Stuttgart (1994).
- R. Taylor and D. R. M. Walton, *Nature* 363, 685 (1993).
- A. Hirsch, *Angew. Chem., Int. ED Engl.* 32, 1138 (1993).
- A. Hirsch, *J. Phys. Chem. Solids* 58, 1729 (1997).
- A. Hirsch, *Synthesis* 1995, 895 (1995).
- A. W. Jensen, S. R. Wilson, and D. I. Schuster, *Biorg. Med. Chem.* 4, 767 (1996).
- F. Diederich and C. Thilgen, *Science* 271, 317 (1996).
- B.-X. Chen, S. R. Wilson, M. Das, D. J. Coughlin, and B. F. Erlanger, *Proc. Natl. Acad. Sci. U.S.A.* 95, 10809 (1998).
- T. D. Ros and M. Prato, *Chem. Commun.* 663 (1999).
- Y. He and Y. Li, *Phys. Chem. Chem. Phys.* 13, 1970 (2011).
- A. Hirsch and B. Nuber, *Acc. Chem. Res.* 32, 795 (1999).
- N. F. Gol'dshleger and A. P. Moravskii, *Russ. Chem. Rev.* 66, 323 (1997).
- R. G. Bergosh, M. S. Meier, J. A. L. Cooke, H. P. Spielmann, and B. R. Weedon, *J. Org. Chem.* 62, 7667 (1997).
- A. L. Balch and M. M. Olmstead, *Chem. Rev.* 98, 2123, (1998).
- B. I. Kharisov, O. V. Kharissova, M. J. Gomez, and U. O. Mendez, *Ind. Eng. Chem. Res.* 48, 545 (2009).
- D. M. Guldi, C. Luo, and A. Swartz, *J. Org. Chem.* 67, 1141 (2002).
- J. L. Bredas, R. Silbey, D. S. Boudreaux, and R. R. Chance, *J. Am. Chem. Soc.* 105, 6555 (1983).
- Y. Z. Lee, X. W. Chen, S. A. Chen, P. K. Wei, and W. S. Fann, *J. Am. Chem. Soc.* 123, 2296 (2001).

Received: 7 November 2011. Accepted: 27 March 2012.